

## Supplementary Information

### $\text{Mg}_3(\text{Bi,Sb})_2$ single crystals towards high thermoelectric performance

Yu Pan,<sup>\*a†</sup> Mengyu Yao,<sup>a†</sup> Xiaochen Hong,<sup>b</sup> Yifan Zhu,<sup>c,d</sup> Fengren Fan,<sup>a</sup> Kazuki Imasato,<sup>e</sup> Yangkun He,<sup>a</sup> Christian Hess,<sup>b</sup> Jörg Fink,<sup>a,b,f</sup> Jiong Yang,<sup>c</sup> Bernd Büchner,<sup>b,f</sup> Chenguang Fu,<sup>\*a</sup> G. Jeffrey Snyder,<sup>e</sup> and Claudia Felser<sup>a</sup>

<sup>a</sup>Max Planck Institute for Chemical Physics of Solids, Nöthnitzer Str. 40, 01187, Dresden, Germany. \*E-mail: [yu.pan@cpfs.mpg.de](mailto:yu.pan@cpfs.mpg.de); [chenguang.fu@cpfs.mpg.de](mailto:chenguang.fu@cpfs.mpg.de)

<sup>b</sup>Leibniz-Institute for Solid State and Materials Research (IFW-Dresden), Helmholtzstraße 20, 01069, Dresden, Germany.

<sup>c</sup>Materials Genome Institute, Shanghai University, 99 Shangda Road, Shanghai 200444, China.

<sup>d</sup>State Key Laboratory of High Performance Ceramics and Superfine Microstructure, Shanghai Institute of Ceramics, Chinese Academy of Sciences, Shanghai 200050, China.

<sup>e</sup>Department of Materials Science and Engineering, Northwestern University, Evanston, IL 60208, USA.

<sup>f</sup>Institute for Solid-State and Materials Physics, Technical University Dresden, 01062 Dresden, Germany

<sup>†</sup>These authors contributed equally.

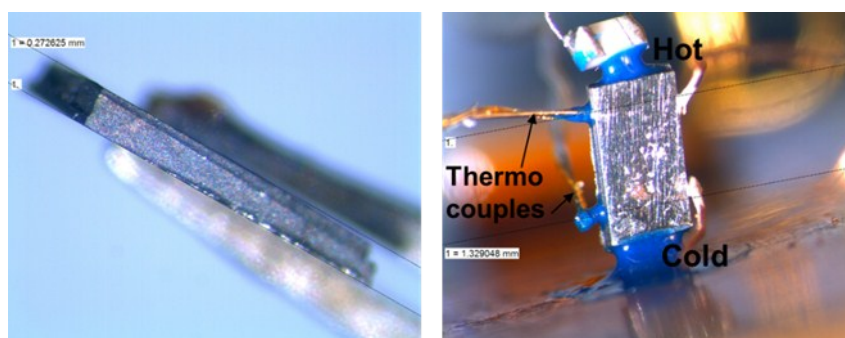


**Fig. S1** Sample setup for thermal conductivity measurement by steady state method. Thermal gradient is along the *ab* plane direction (parallel to the layered plane of the single crystals).

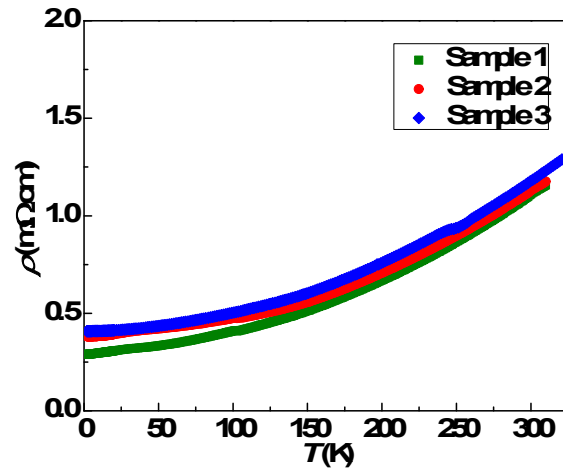


**Fig. S2** Temperature dependence of the resistivity for three samples from the same batch of Y-doped  $\text{Mg}_3\text{Bi}_{1.25}\text{Sb}_{0.75}$  single crystals.

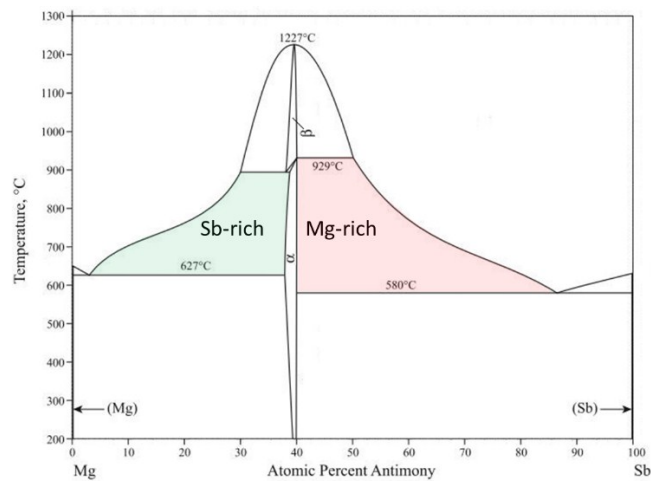


**Fig. S3** Phase diagram of Mg-Sb.

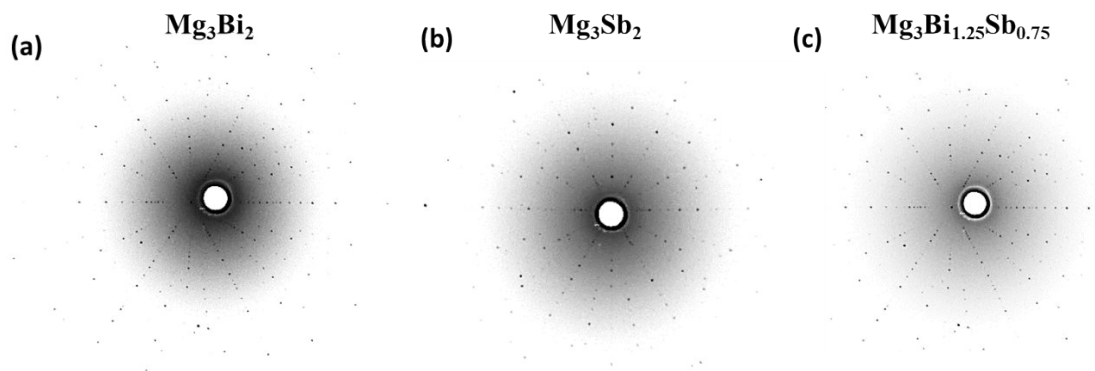


**Fig. S4** (a)-(c) Laue XRD pattern of  $\text{Mg}_3\text{Bi}_2$ ,  $\text{Mg}_3\text{Sb}_2$  and  $\text{Mg}_3\text{Bi}_{1.25}\text{Sb}_{0.75}$ , respectively.

For all three single crystals, the backscattering Laue XRD diffraction patterns show clear diffraction spots, and no impurity dots are found, indicating the high quality and crystallinity of the as-grown single crystals.

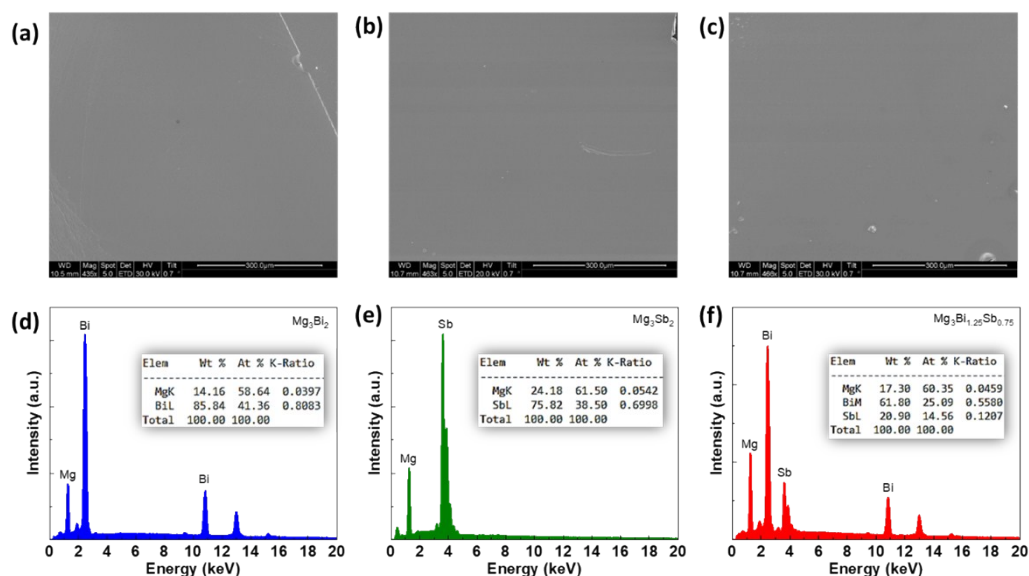


**Fig. S5** (a)-(c) SEM images and (d)-(f) EDX patterns of  $Mg_3Bi_2$ ,  $Mg_3Sb_2$  and  $Mg_3Bi_{1.25}Sb_{0.75}$ , respectively.

SEM with EDX analysis demonstrates the chemical compositions of  $Mg_3Bi_2$  and  $Mg_3Sb_2$  agree well with the stoichiometric compositions (**Fig. S5**). The ternary compound is revealed to be  $Mg_3Bi_{1.25}Sb_{0.75}$  according to the EDX analysis. It is worth noting that the compositions of the single crystals are very close to the Mg : X = 3 : 2 relation (X = Bi, Sb) without an uncontrollable large amount of excess Mg as in polycrystalline samples.

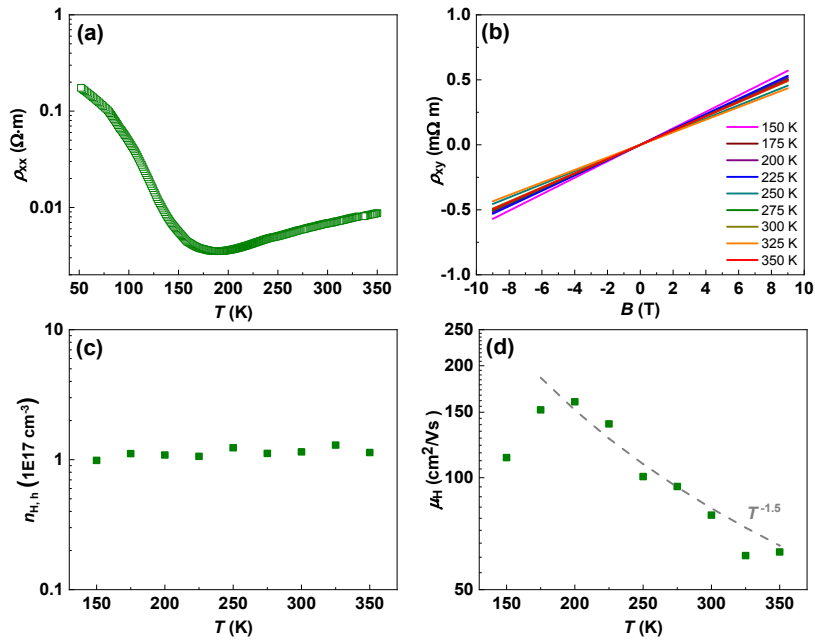


**Fig. S6** Electrical transport properties of  $\text{Mg}_3\text{Sb}_2$ . (a) Temperature dependence of resistivity, (b) magnetic field dependence of Hall resistivity, (c) Hall carrier concentration, (d) Hall mobility.

Pure  $\text{Mg}_3\text{Sb}_2$  show a semiconducting behavior with a first decrease and then increase resistivity with increasing temperature, as shown in **Fig. S6(a)**. As a semiconductor, the pure  $\text{Mg}_3\text{Sb}_2$  sample show very high resistivity, demonstrating the high quality of the single crystal. Linear magnetic field dependence of the Hall resistivity with a positive slope indicates the p-type transport behavior of the sample. The hole concentration is pretty low and hardly changes in the whole temperature range. The mobility shows a  $T^{-1.5}$  dependence which implies the dominant scattering as phonon scattering. Although  $\text{Mg}_3\text{Sb}_2$  shows a p-type behavior, the single crystals can be doped into n-type since they are rich of Mg.

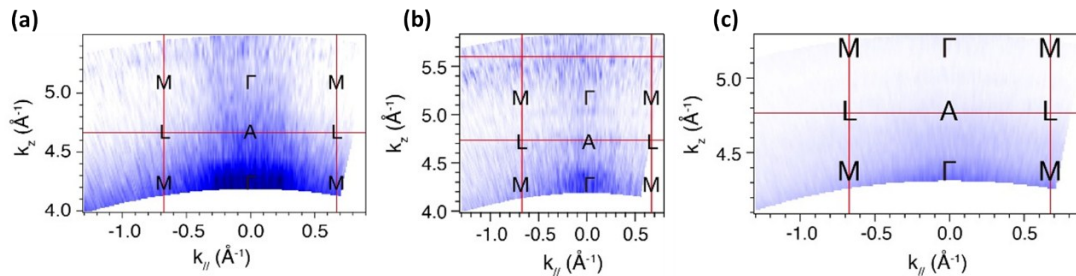


**Fig. S7** ARPES intensity at different  $k_z$ . (a)  $\text{Mg}_3\text{Bi}_2$ , (b)  $\text{Mg}_3\text{Bi}_{1.25}\text{Sb}_{0.75}$ , (c)  $\text{Mg}_3\text{Sb}_2$ .

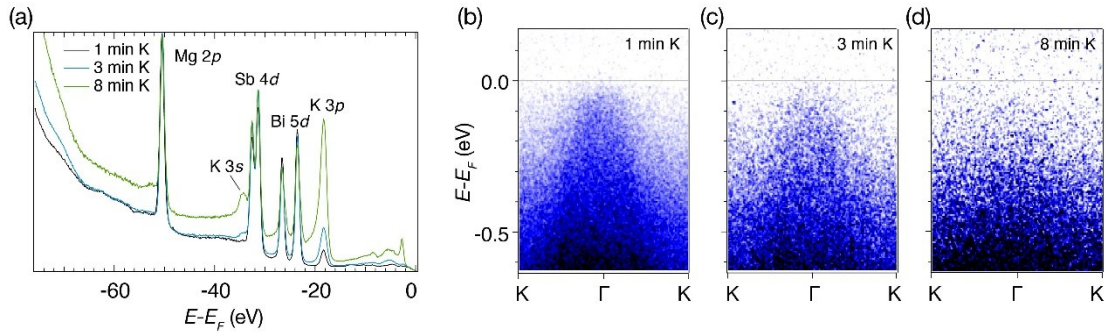


**Fig. S8** K-doped  $\text{Mg}_3\text{Bi}_{1.25}\text{Sb}_{0.75}$  photoemission. (a) K-doped  $\text{Mg}_3\text{Bi}_{1.25}\text{Sb}_{0.75}$  core-level spectra, obtained with  $h\nu = 95$  eV. (b)-(d) Series of ARPES intensity plots along  $\Gamma$ -K.

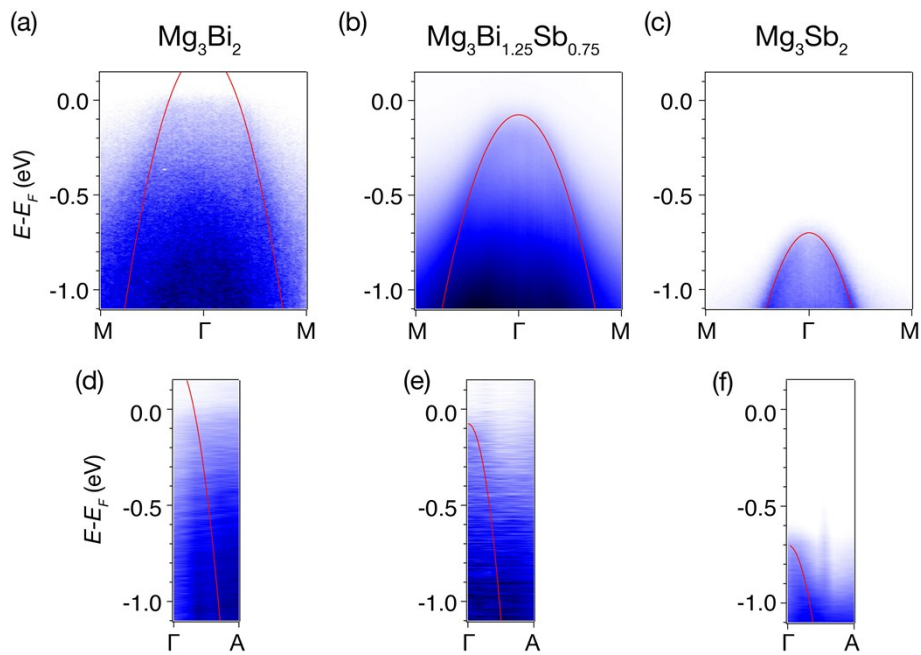


**Fig. S9** ARPES intensity plots of three compounds along high symmetry directions, (a)-(c)  $\Gamma$ -M, (d)-(f)  $\Gamma$ -A. The red lines are parabolic fitting lines.

The effective mass can be calculated by fitting the band dispersions with parabola. As shown in **Fig. S9**, we fit the hole bands of the three compounds along the  $\Gamma$ -M and  $\Gamma$ -A directions. Effective mass values of  $\text{Mg}_3\text{Bi}_2$  are  $0.72 m_e$  and  $0.24 m_e$  along in-plane ( $\Gamma$ -M) and cross-plane ( $\Gamma$ -A) directions, respectively.  $\text{Mg}_3\text{Sb}_2$  shows  $0.9 m_e$  and  $0.16 m_e$  and  $\text{Mg}_3\text{Bi}_{1.25}\text{Sb}_{0.75}$  shows  $0.72 m_e$  and  $0.24 m_e$  along in-plane and cross-plane directions, respectively.